Supporting information

Highly efficient solar to chemical conversion by anthraquinone and *Candida antarctica* lipase B based photocatalytic-enzymatic Cascade

Yuting Li[a, b], Jie Cheng[b], Yinghuan Xu[b], Jiacan Zhu[a], Xiahui Huang[b], Pengcheng Zhang[b], Hongzhang Wu[d], Zhenjiang Cao[c*], Jianbo Zhao[a*], Kaipeng Cheng[b*]

a School of Chemistry and Chemical Engineering, Tarim University, Alar 843300, PR China

b School of Chemistry and Chemical Engineering, Zhoukou Normal University, Zhoukou 466000, PR China

b School of Chemistry and Chemical Engineering, Tarim University, Alar 843300, PR China

c School of Chemistry, Xi'an Jiaotong University, Xi'an 710049, PR China

d Henan Key Laboratory of Rare Earth Functional Materials and Application, Zhoukou Normal University, Zhoukou 466000, PR China

Experimental Section

Materials

Zinc Nitrate Hexahydrate, 2-Methylimidazole, Sodium anthraquinone-2-sulfonate (SAS), (-)-Limonene, (+)-Limonene 1,2-epoxide and 2, 2'-azino-bis(3-ethylbenzothiazoline-6-sulfonic acid) (ABTS) were purchased from Shanghai Macklin Biochemical Co., Ltd. Horseradish Peroxidase (HRP, ≥300u/mg) was purchased from Shanghai yuanye Bio-Technology Co., Ltd. *Candida antarctica* lipase B (CALB, 10000U/mg, liquid) was purchased from Novozymes. All chemicals were used without further processing.

ZIF-8 Synthesis

ZIF-8 was synthesized as references reported with slightly differences[1]. Typically, 0.2 mL of $Zn(NO_3)_2$ solution (0.31 M) was simultaneously added into 2 mL of 2-methylimidazole solution (1.25 M) and then stirred thoroughly at room temperature for 12 h. ZIF-8 was collected by centrifugation followed by methanol washing for 3 times, and was dried under vacuum at 80 ºC for 12 h.

SAS@ZIF-8 Synthesis

SAS was added into 2 mL of 2-methylimidazole solution (1.25 M), and was stirred until fully dissolved. Then 0.2 mL of $Zn(NO_3)_2$ solution (0.31 M) was simultaneously added into the above mixture, and then stirred thoroughly at room temperature for 12 h. SAS@ZIF-8 was collected by centrifugation followed by methanol washing for 3 times, and was dried under vacuum at 80 ºC for 12 h (Yield: 90 mg). The SAS concentration in the reactant range from 1.25 to 40 mM, and the encapsulation efficiency was obtained according to residue amount in supernatant by reading absorbance at 327 nm using UV-Vis spectrophotometer.

SAS-CALB@ZIF-8 Synthesis

SAS was added into 2 mL of 2-methylimidazole solution (1.25 M) and CALB was added into 0.2 mL of $Zn(NO_3)_2$ solution (0.31 M). The mixtures were stirred until fully dissolved. Then, the later mixture was simultaneously added into the former mixture and kept stirring for 12 h at room temperature. The solid was collected by centrifugation followed by washing using PBS buffer (pH = 7, 50 mM) for 3 times, and was

redispersed in 2 mL PBS buffer at 4 ºC for further using. The SAS concentration in the reactant was 20 mM, and CALB dosage differ from 20 to 200 μL. HPLC equipped with C18 column and UV detector was used here to measure the residue CALB in supernatant of first round centrifugation.

Photocatalytic Reaction

The photocatalytic H_2O_2 production performance of various catalysts was evaluated under white light irradiation using CEL-PCRD300-12 (Beijing China Education Au-Light Technology Co Ltd.) equipped with LED lamp beads, cooling fan, and power conditioner.

Typically, 4 mg SAS@ZIF-8 or equivalent SAS was dispersed or dissolved in O_2 saturated water. The mixture was irradiated for 4 h with stir, and samples were collected every hour to test the H_2O_2 accumulation amount by enzymatic approach. For each test run, 50 μL sample after centrifugation and dilution, 50 μL ABTS (50 mM) and 50 μL HRP (1 mg/mL) were added into 850 μL PBS, and then shook for 5 min. UV-Vis spectrophotometer was used to read the absorbance at 419 nm, and the yield can be obtained according to the standard curve. For scavenger experiments, $AgNO_3$, BQ or TBA was added in the reactant with concentration of 10 mM.

Photo-Enzymatic Cascade

SCZ photo-enzymatic cascade: SCZ was stored in PBS at 4 ºC before using as described above. Typically, 500 μL SCZ, ethyl acetate (3 M), isopropanol (25 v/v %) and limonene (0.1 M) were added into O_2 saturated PBS (pH = 7.0, 50 mM) with final volume of 4 mL. After irradiation for 1 h, 200 μL mixture was collected followed by adding 160 μL ethanol solution of n-dodecane (1/20000 v/v, as internal standard and to quench the reaction). GC equipped with FID detector was used here to measure the limonene oxide yield.

CALB + H_2O_2: Equivalent CALB (50 μL), H_2O_2 (2.5 mM according to the H_2O_2 accumulation amount using SCZ), ethyl acetate (3 M), isopropanol (25 v/v %) and limonene (0.1 M) were added into O_2 saturated PBS (pH = 7.0, 50 mM) with final volume of 4 mL. The reaction started with all chemicals added, and lasted for 1 h.

CALB@ZIF-8 + SAS: 500 μL SCZ, SAS, ethyl acetate (3 M), isopropanol (25 v/v %)

and limonene (0.1 M) were added into O_2 saturated PBS (pH = 7.0, 50 mM) with final volume of 4 mL. The reaction started by turning on light, and lasted for 1 h.

CALB + SAS@ZIF-8-20: 8 mg SAS, equivalent CALB (50 μL), ethyl acetate (3 M), isopropanol (25 v/v %) and limonene (0.1 M) were added into O_2 saturated PBS (pH = 7.0, 50 mM) with final volume of 4 mL. The reaction started by turning on light, and lasted for 1 h.

CALB + SAS: equivalent CALB (50 μL), SAS, ethyl acetate (3 M), isopropanol (25 v/v %) and limonene (0.1 M) were added into O_2 saturated PBS (pH = 7.0, 50 mM) with final volume of 4 mL. The reaction started by turning on light, and lasted for 1 h.

DFT Calculation

The reaction path calculations were performed with the projector-augmented-wave (PAW) method as implemented in VASP.[2] The PBE generalized-gradient approximation was adopted for the exchange–correlation functional.[3] A plane-wave basis set was employed with a kinetic-energy cutoff of 400 eV. Owing to the large unit cell of ZIF-8, only the Γ-point was used for Brillouin-zone sampling. Electronic iterations were converged to an energy tolerance of 10^{-8} eV, while the geometry relaxations were considered converged when the maximum force was smaller than 0.02 eV $Å^{-1}$. Gaussian smearing with a width of 0.05 eV was applied during structural optimization.

Characterization

Phase analysis of ZIF-8 and SAS@ZIF-8 series were conducted using D8 ENDEAVOR (Bruker, Germany). The FTIR spectra was recorded using Nicolet iS20 (hermo Fisher Scientific, USA), time resolved photoluminescence decay spectra was recorded using FLS1000 (Edinburgh, UK), EPR spectra was recorded using EMXplus-6/1 (Bruker, Germany), surface morphology was examined using JSM-IT800 (JEOL, Japan). The band gaps and absorption edges were measured using UV-Vis DRS (PerkinElmer Lambda 950, USA).

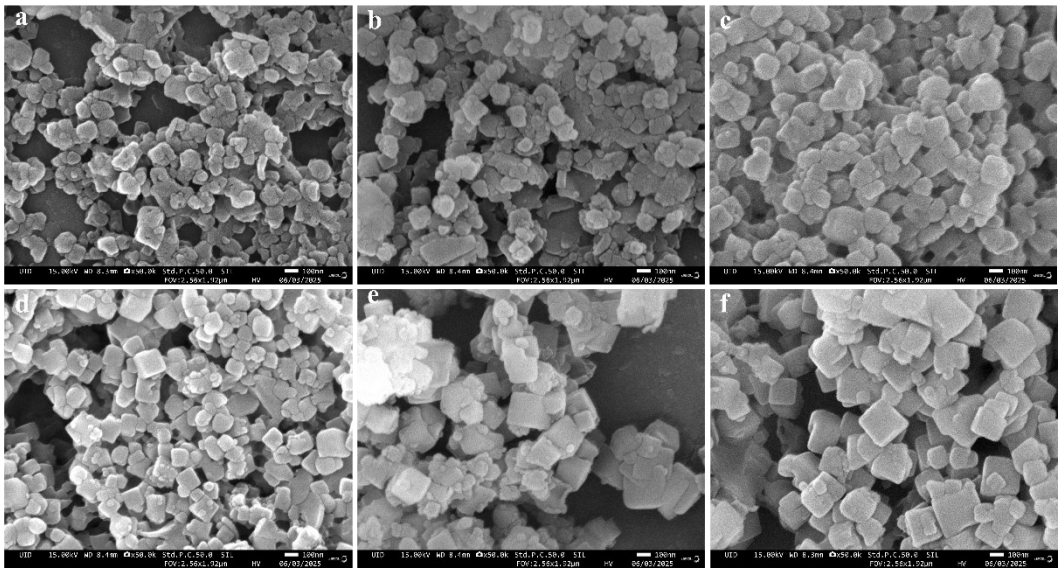

Figure S1: SEM images of SAS@ZIF-8 with different SAS encapsulation amount (a: 40 mM, b: 20 mM, c: 10 mM, d: 5 mM, e: 2.5 mM, f: 1.25 mM)

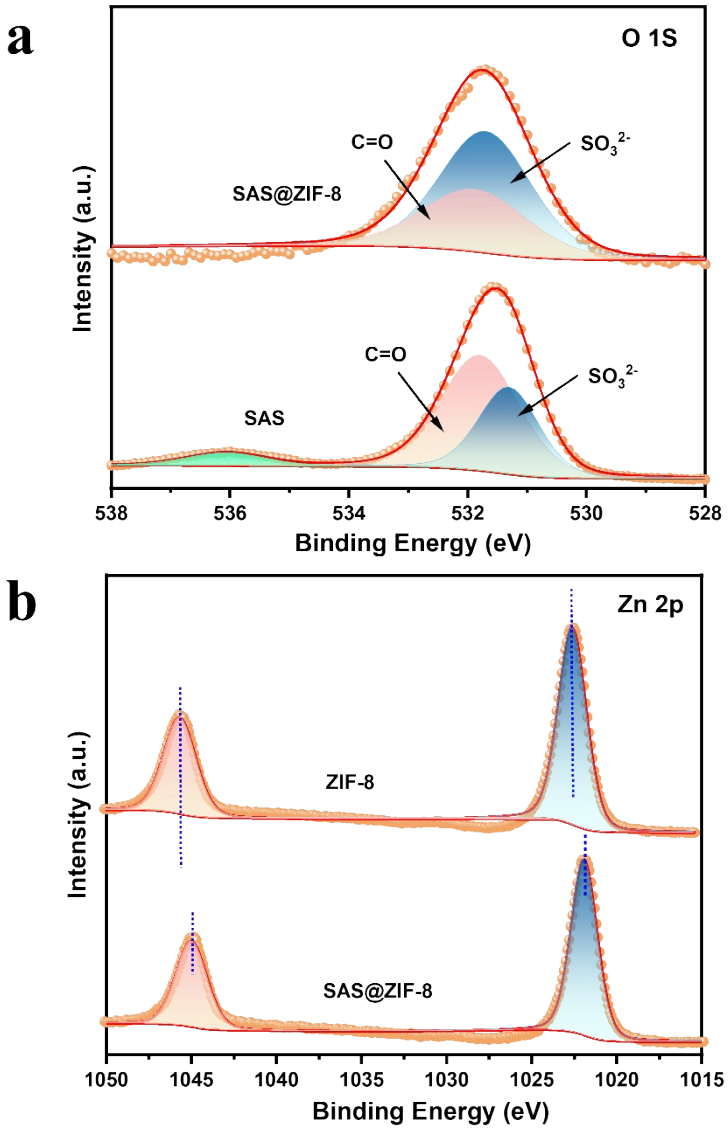

Figure S2: (a) XPS spectra of O 1s orbit of SAS and SAS@ZIF-8, (b) XPS spectra of Zn 2p orbit of ZIF-8 and SAS@ZIF-8.

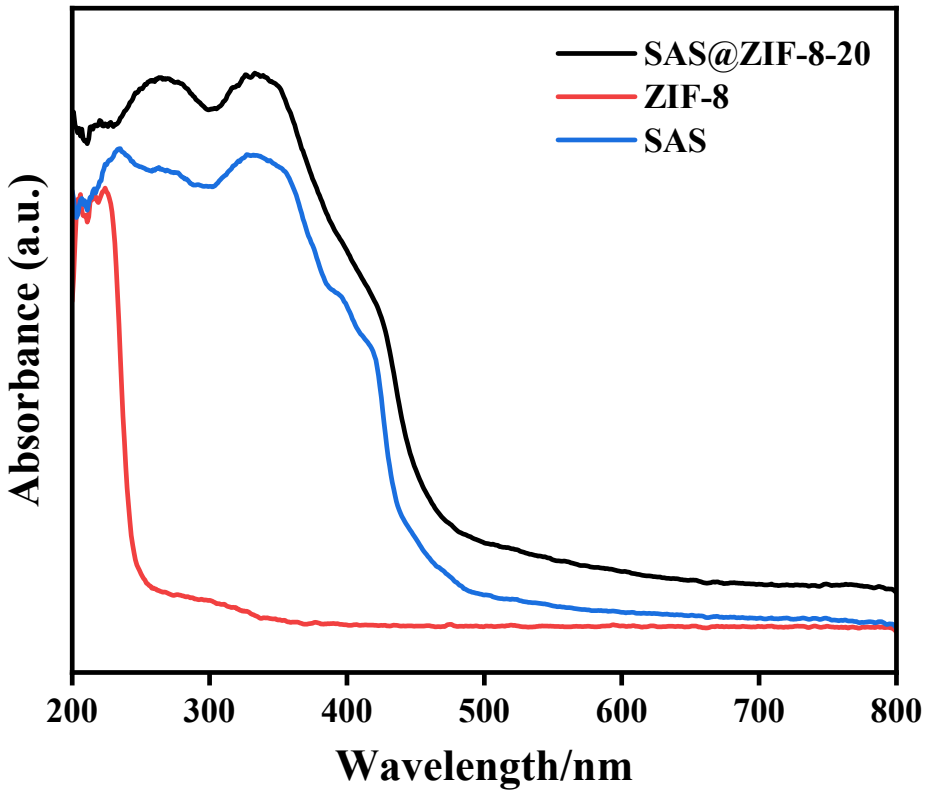

Figure S3: UV-Vis DRS spectra of SAS, ZIF-8 and SAS@ZIF-8.

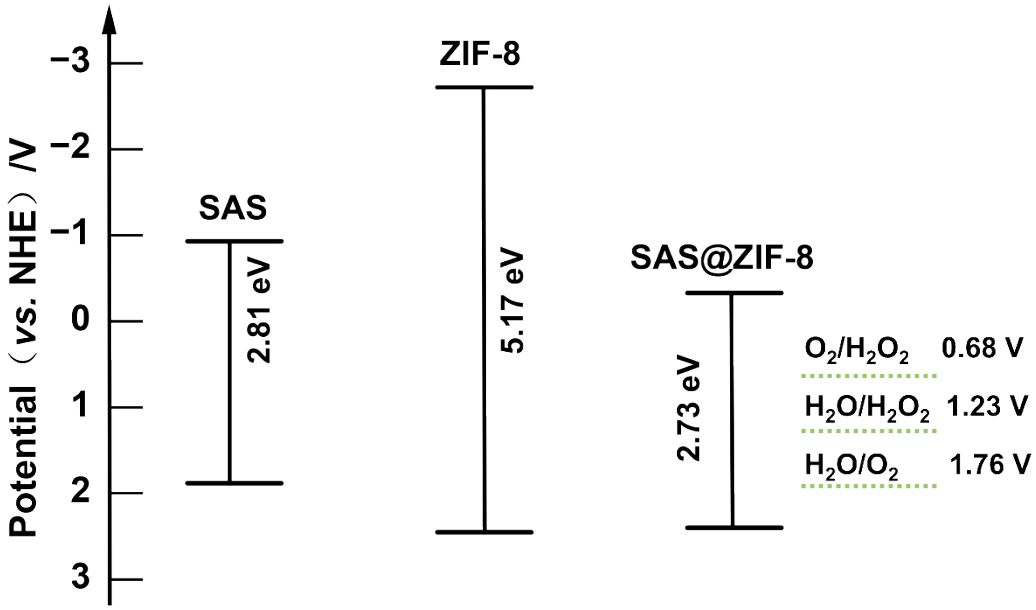

Figure S4: Energy band location of SAS, ZIF-8 and SAS@ZIF-8-20

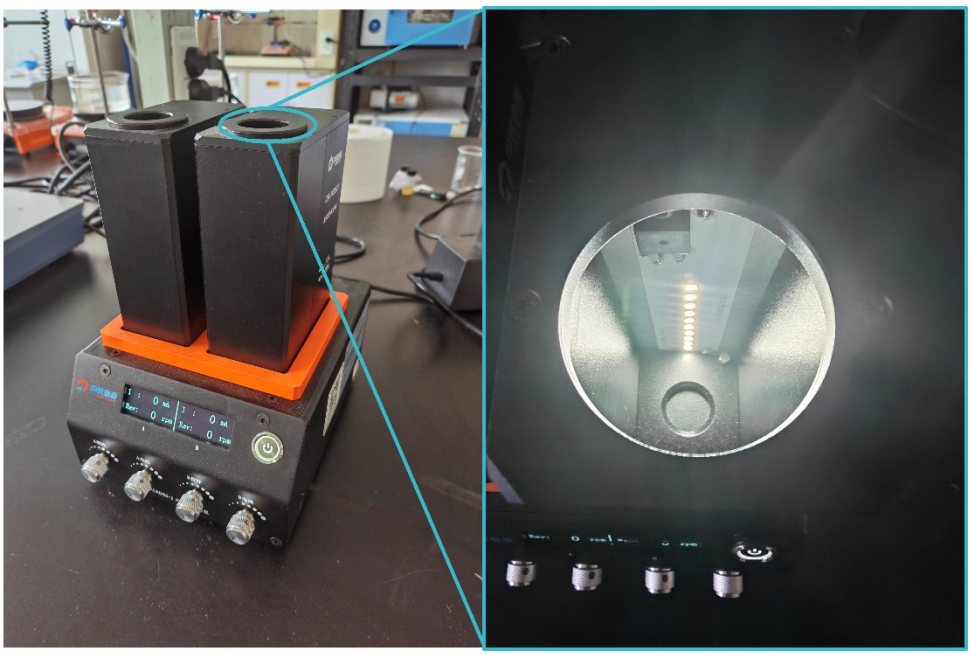

Figure S5: Picture of photocatalytic reactor.

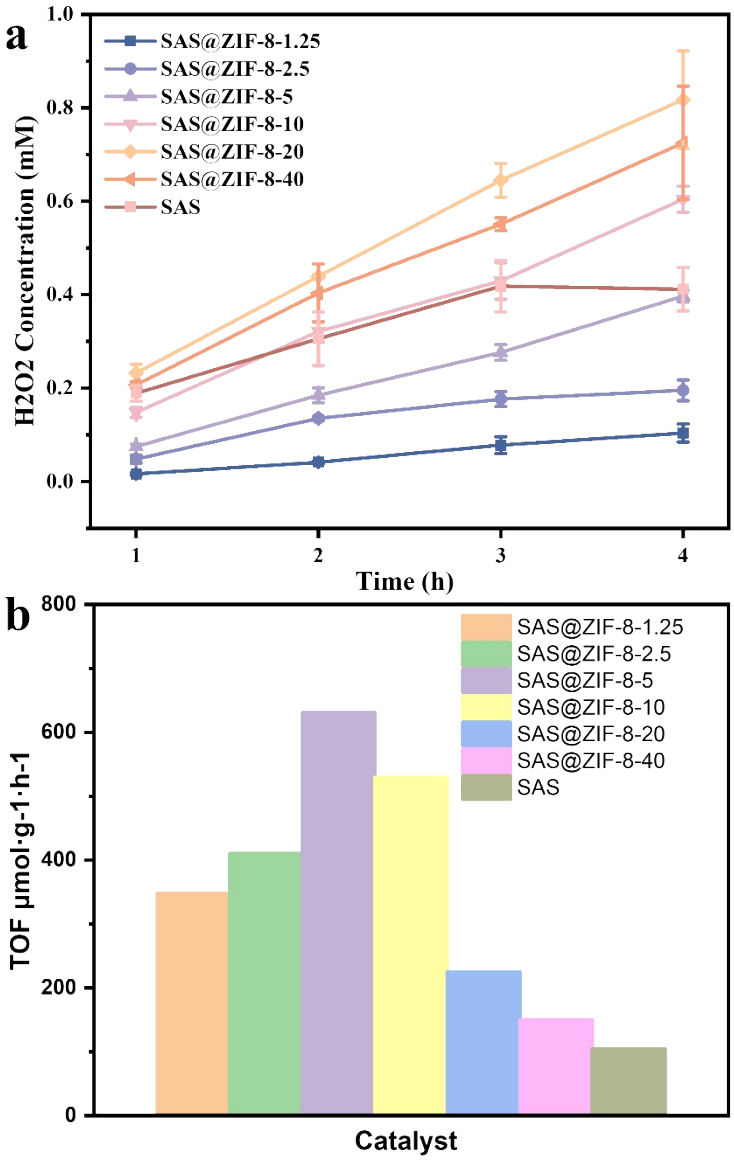

Figure S6: (a)H_2O_2 concentration increasing with time, (b) TOF of SAS@ZIF-8 series and SAS.

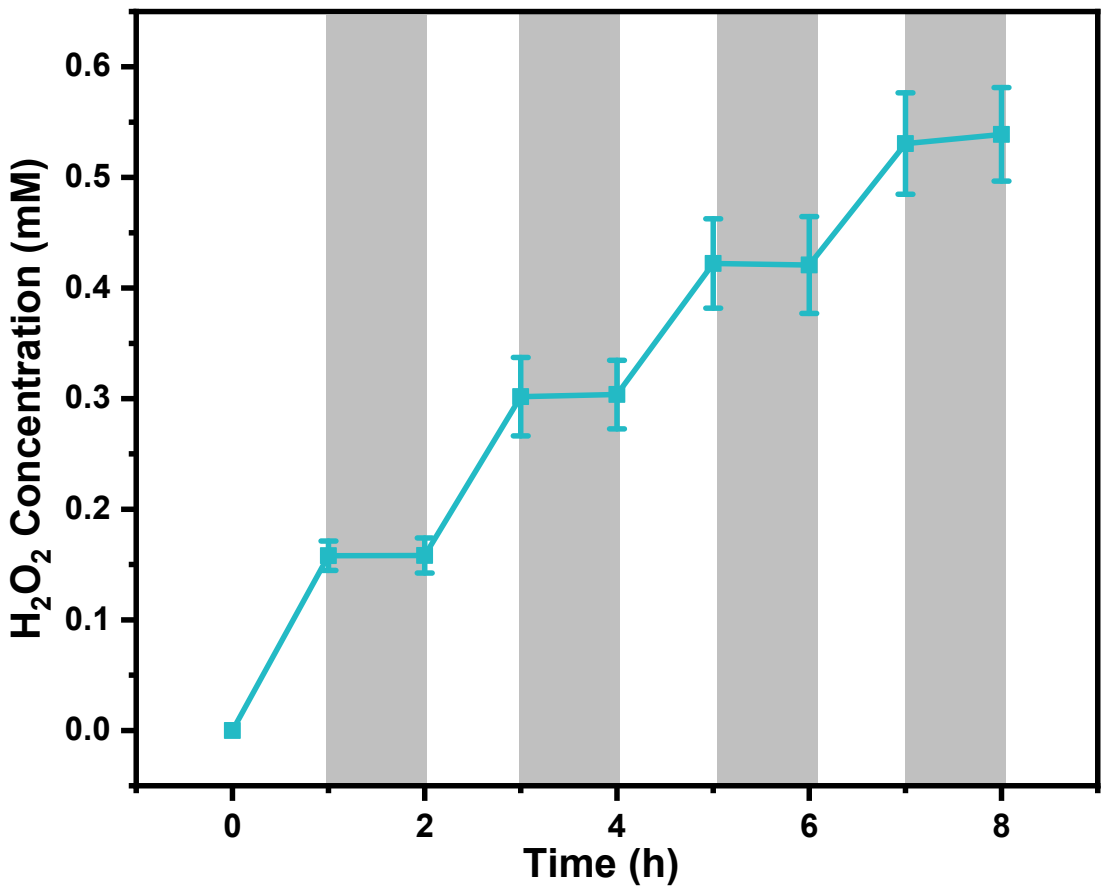

Figure S7: Light on-off cycling with SAS@ZIF-8-20 as catalyst.

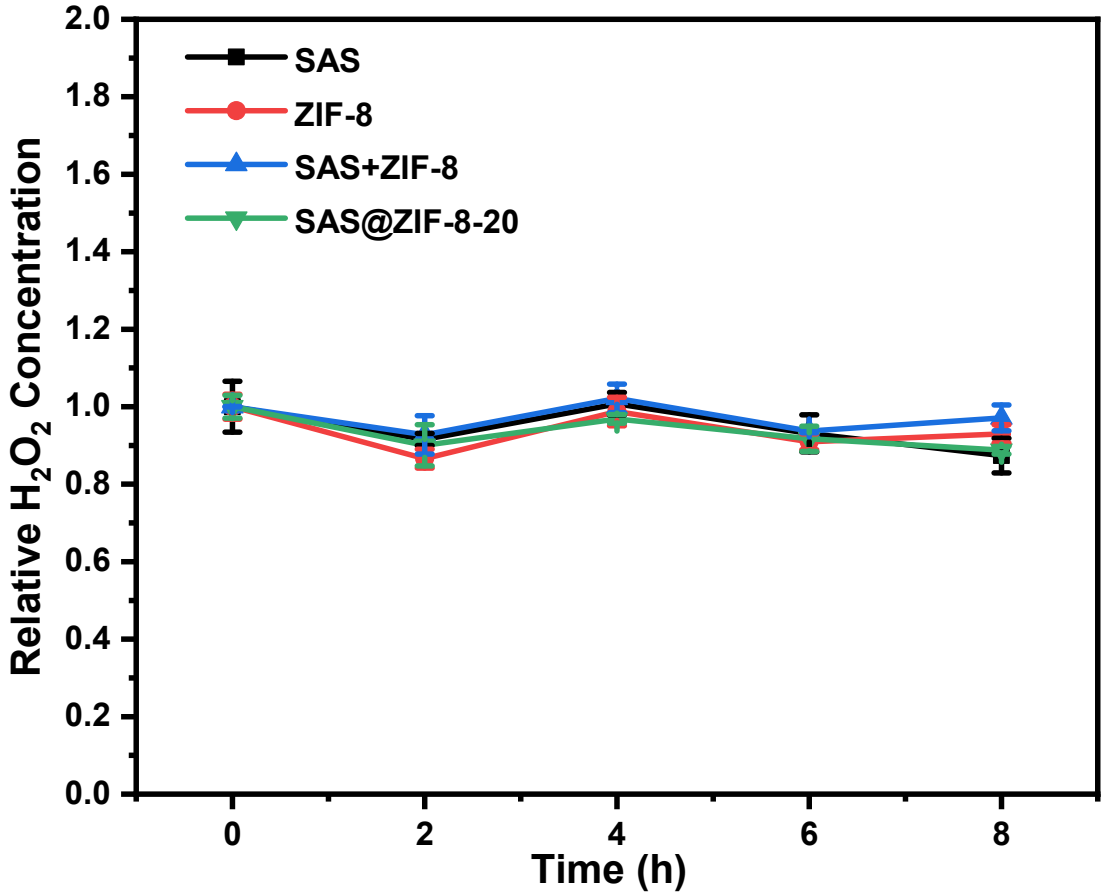

Figure S8: Trace of H_2O_2 content presented with different catalyst

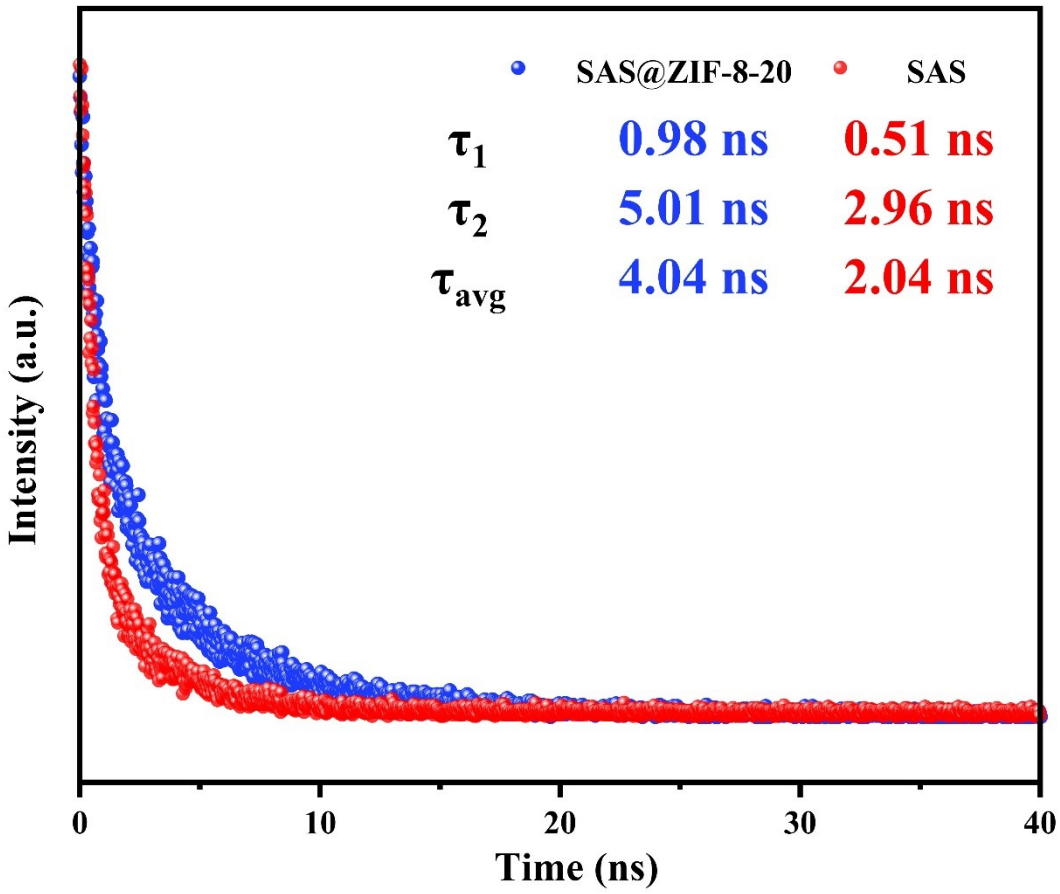

Figure S9: Time resolved photoluminescence decay spectra of SAS and SAS@ZIF-8-20.

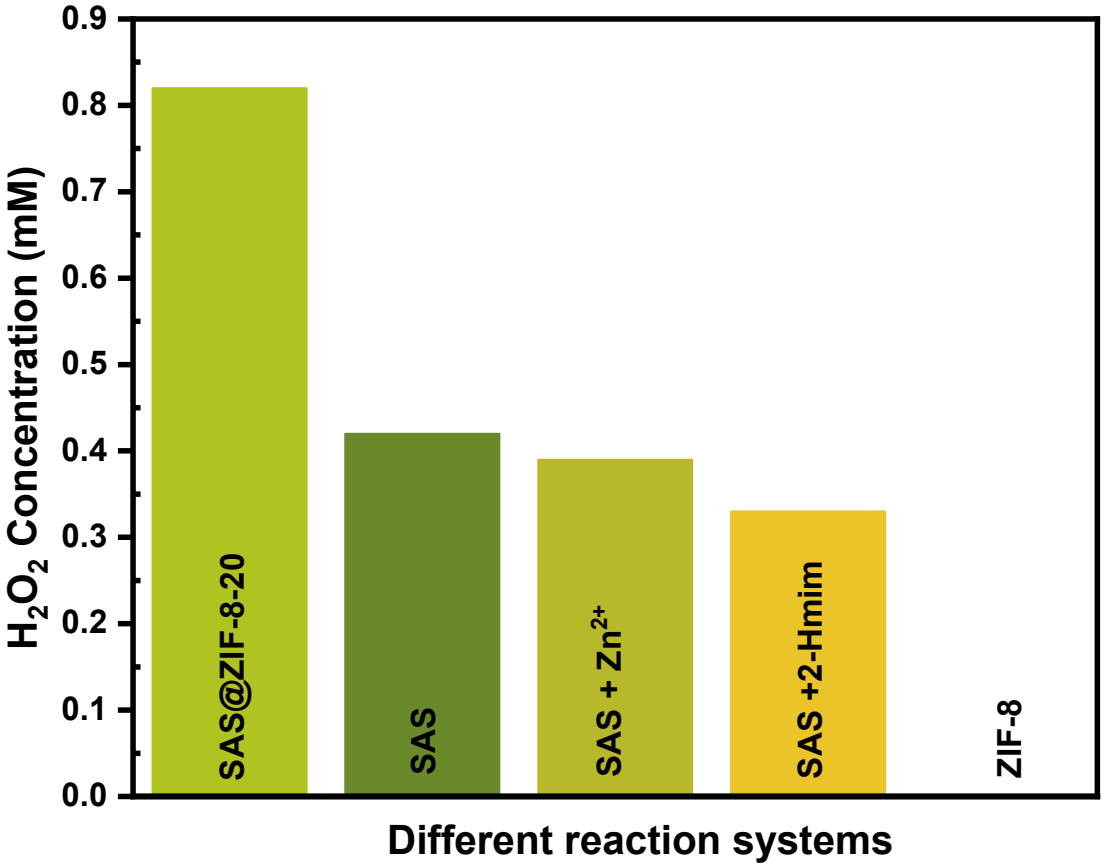

Figure S10: Control experiment of ZIF-8, Zn^{2+} and 2-methylimidazole on H_2O_2 generation

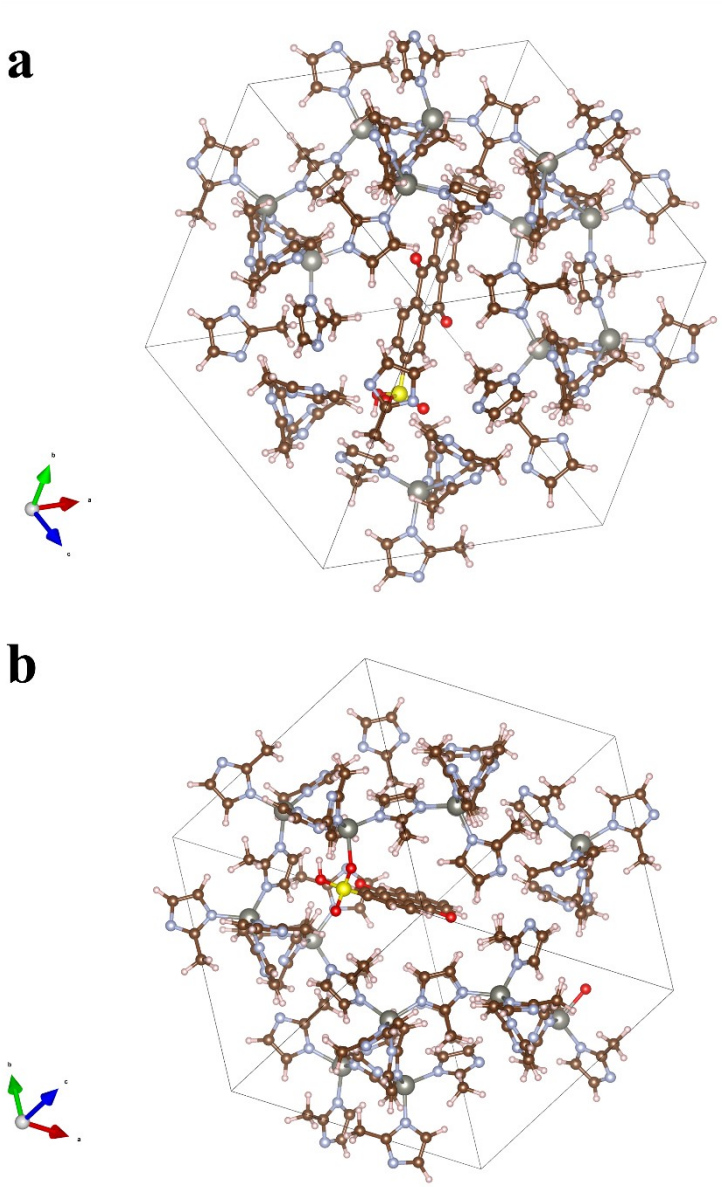

Figure S11: Models of SAS and ZIF-8 composites by physically encapsulation (a) or by interaction (b)

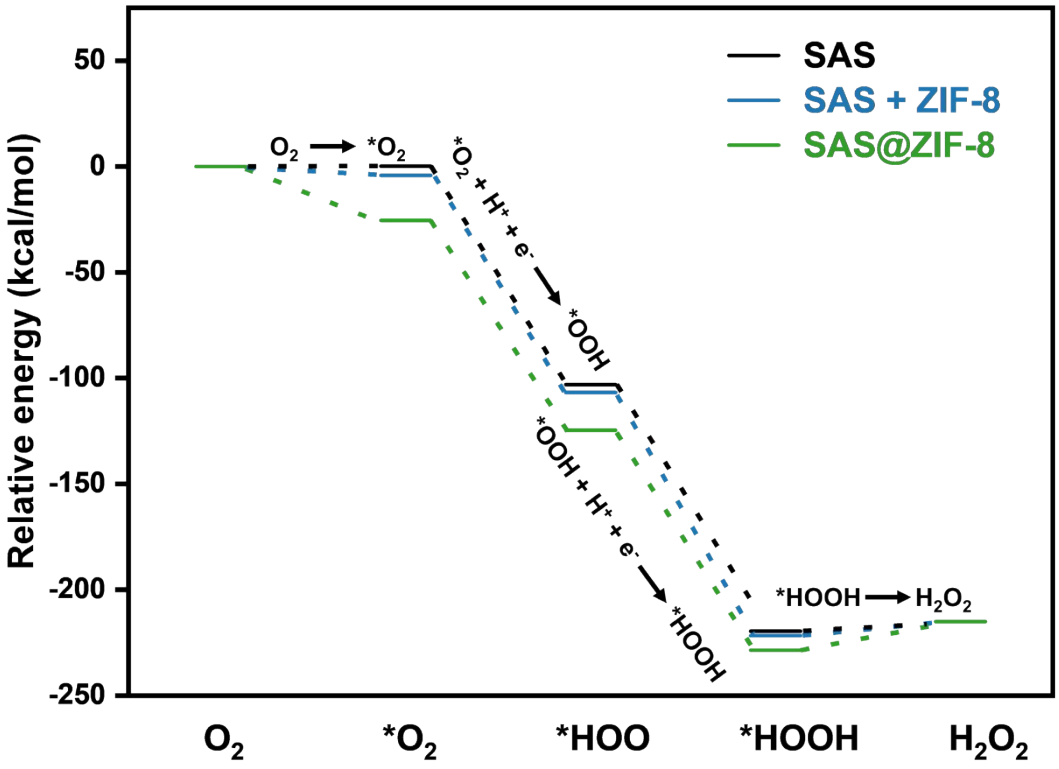

Figure S12: Potential energy diagram describing the O_2-to-H_2O_2 photocatalytic conversion over these three catalysts

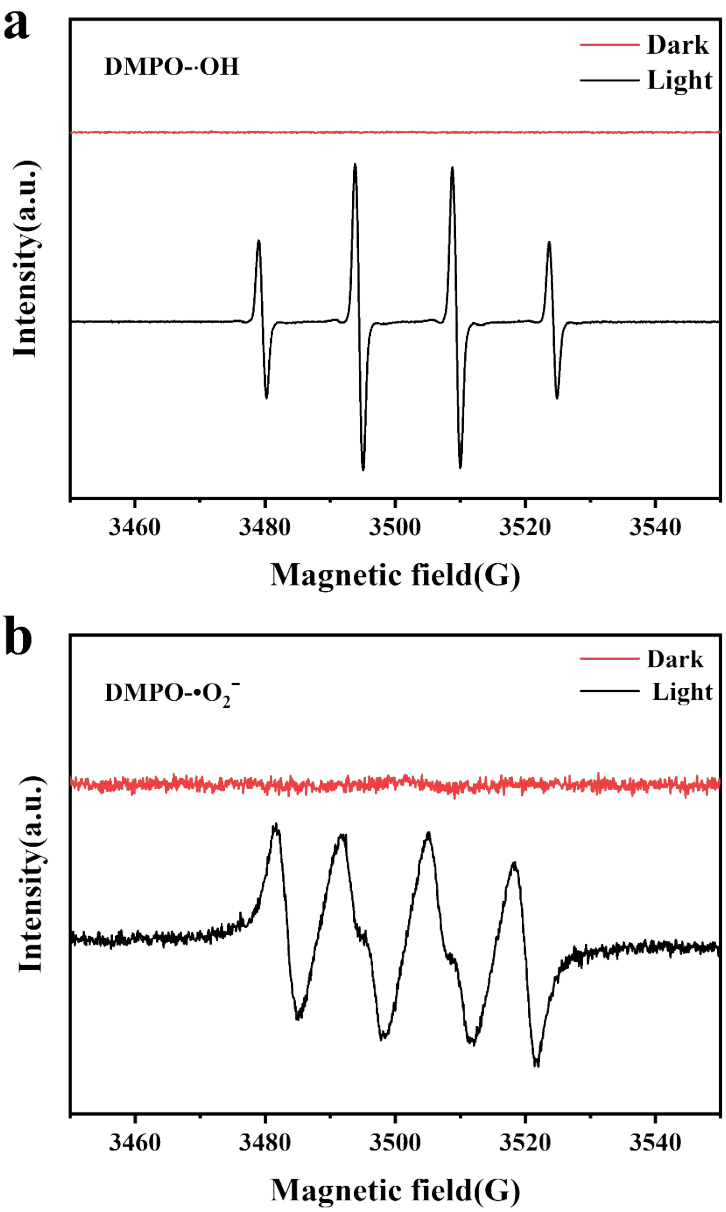

Figure S13: Room-temperature EPR spectra measured with and without light irradiation.

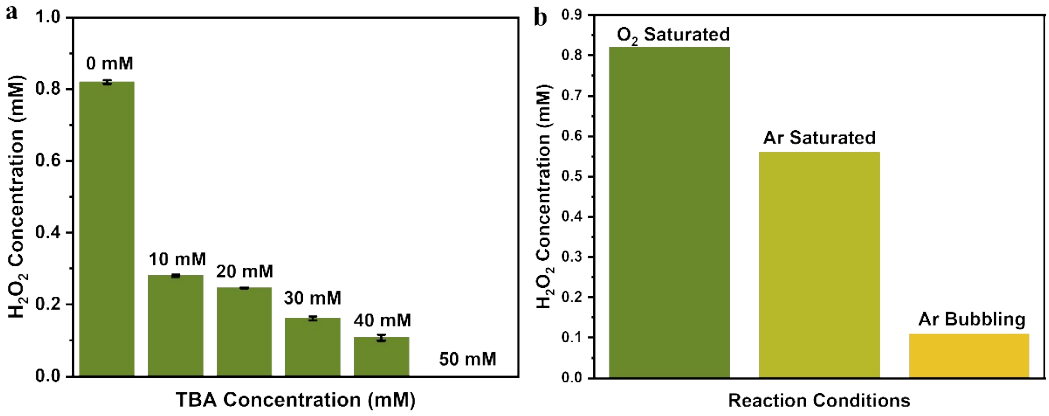

Figure S14: a, Photocatalytic performance under different TBA scavenger amount and Ar Pre-sataurated condition; b, Photocatalytic performance under different atmosphere.

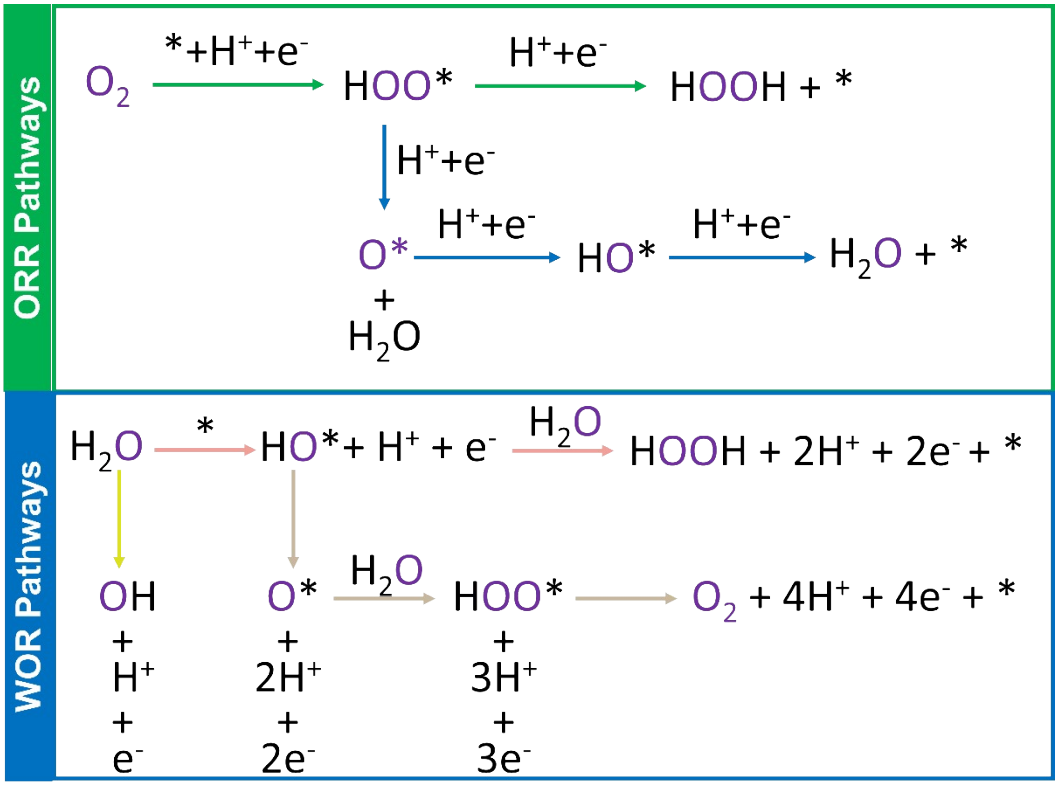

Figure S15: Reaction pathways of 2/4 e^- ORR and 1/2/4 e^- WOR

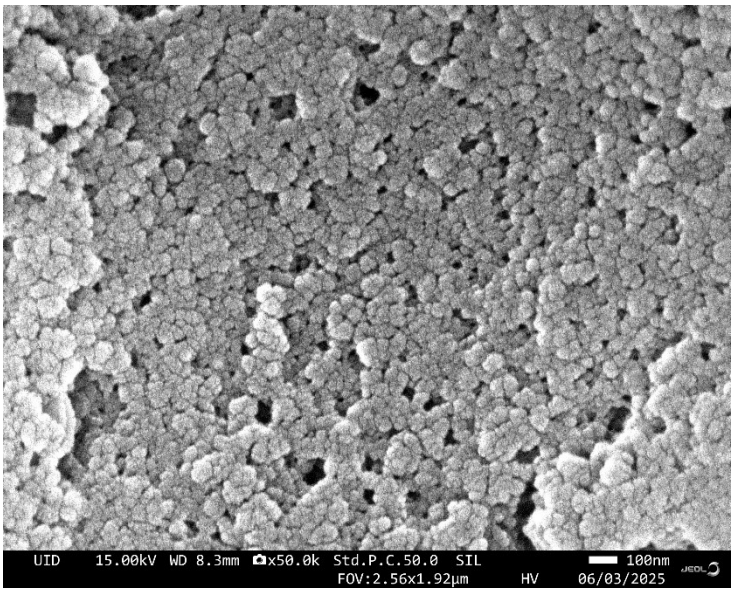

Figure S16: SEM image of SAS-CALB@ZIF-8

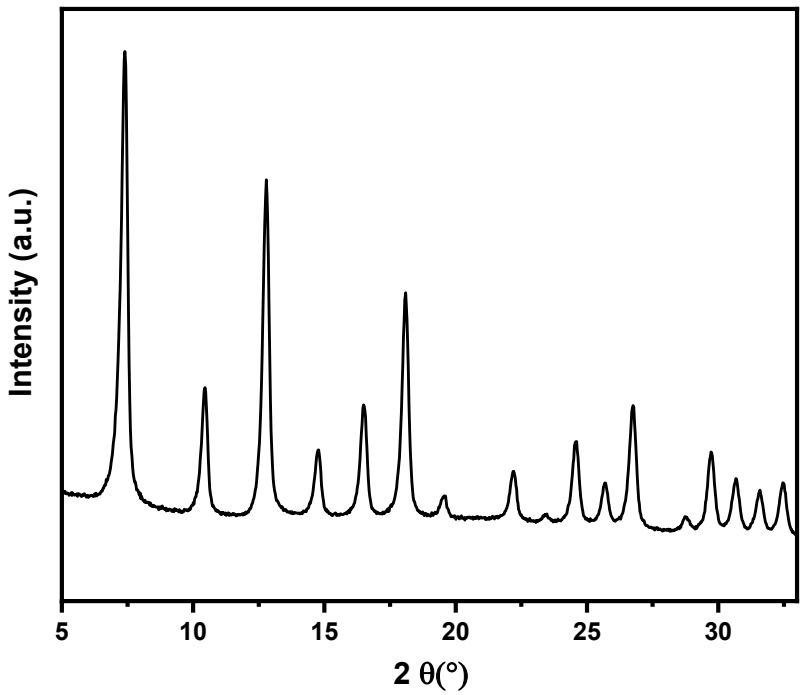

Figure S17: XRD spectra of SAS-CALB@ZIF-8

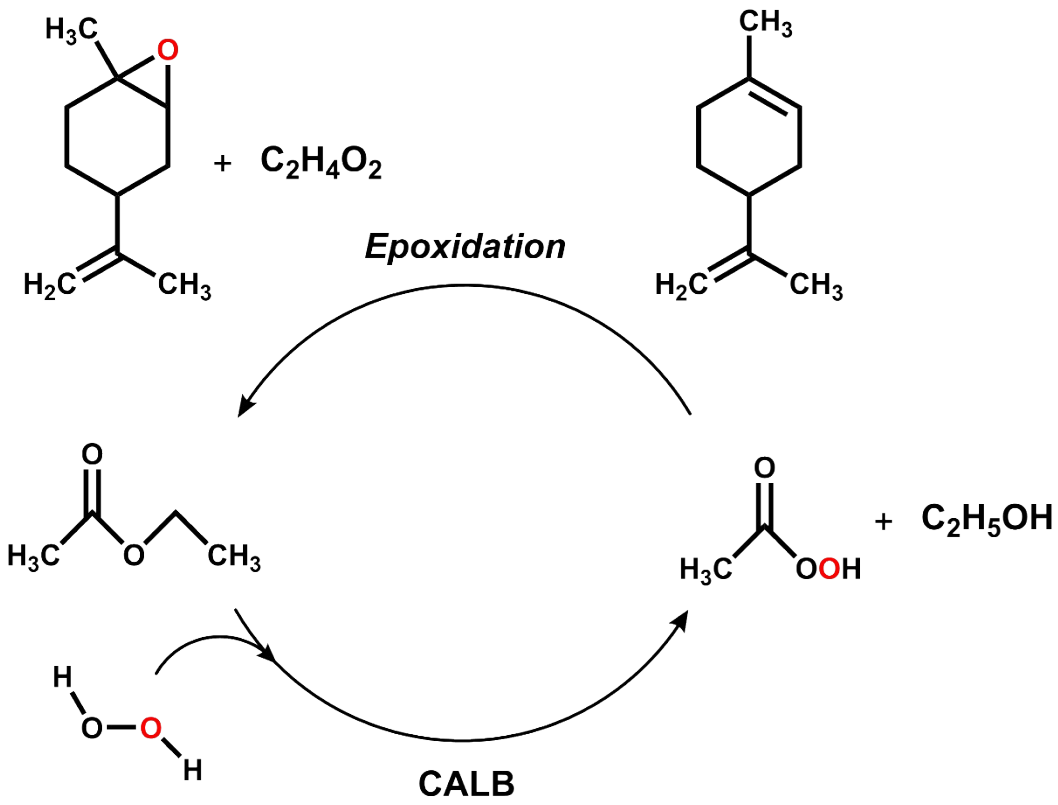

Figure S18: Epoxidation of Limonene driven by CALB and H_2O_2.

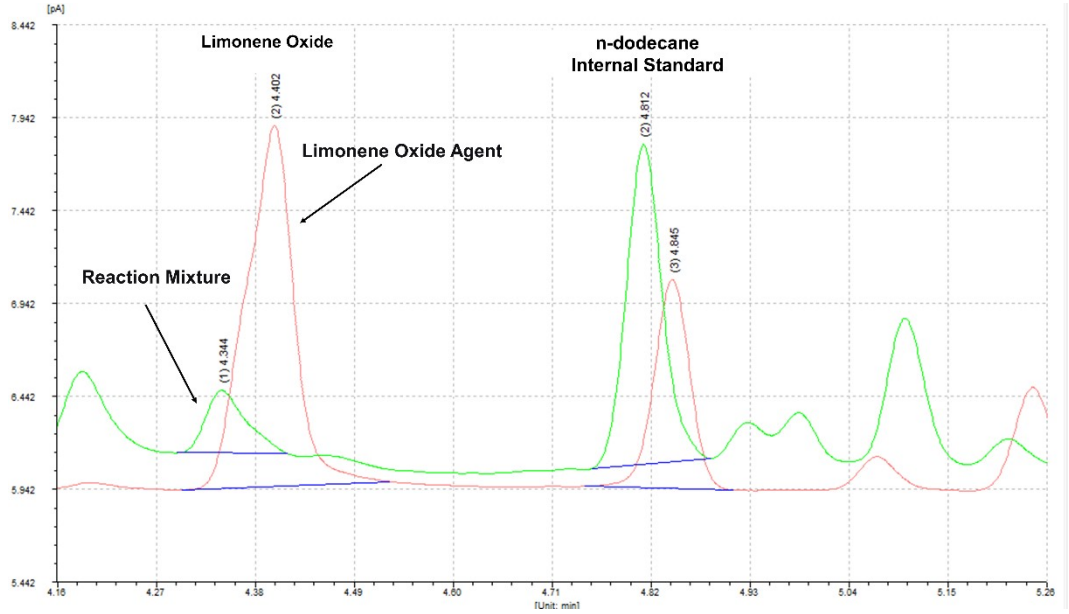

Figure S19: GC spectrum of limonene oxide agent and photo-enzyme catalytic reaction mixture.

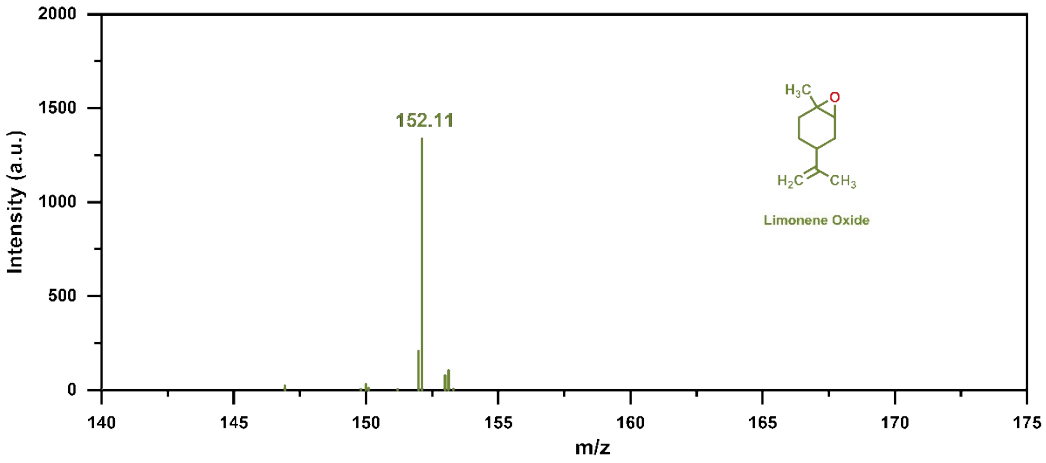

Figure S20: GC-MS spectrum of photo-enzyme catalytic reaction mixture.

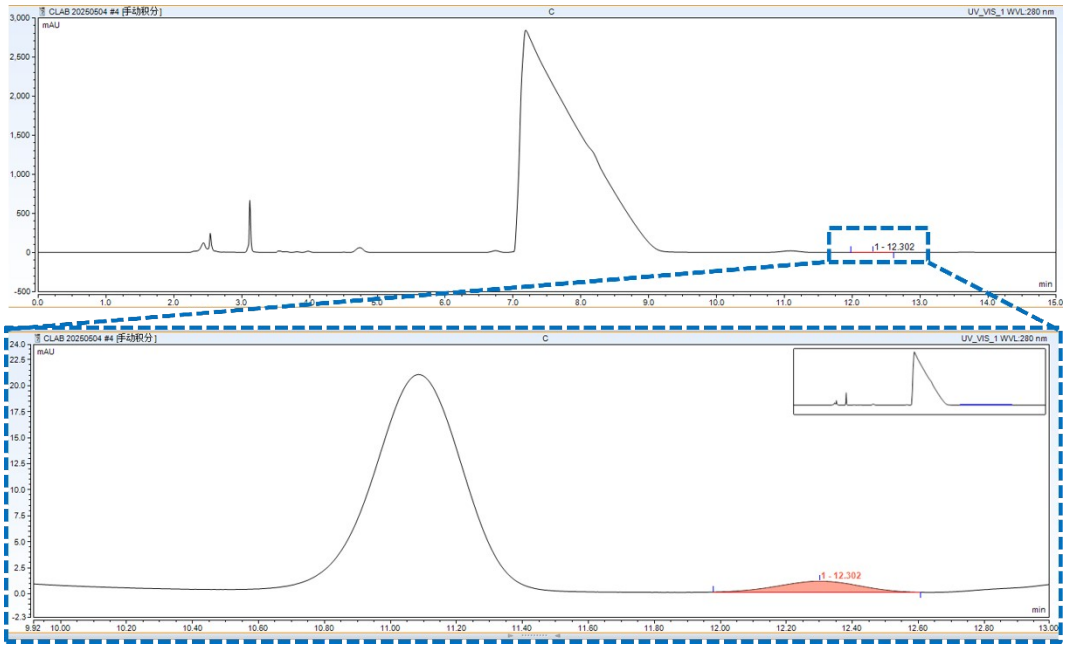

Figure S21: HPLC curves of supernatant during SCZ-200 preparation.

Table S1: TOF comparisons of this work with references

Photo Catalysts	Light	Sacrificial agent	Gas atmosphere	Production rate ($\mu mol \cdot g^{-1} \cdot h^{-1}$)	Production pathway	Ref.
SAS@ZIF-8	Vis		O_2	635	ORR, WOR	This
	Vis	Ethanol	O_2	3556	followed by ORR	Work
C_3N_4/ZIF-8	Vis	No	O_2	2641	ORR, WOR	[4]
MIL-125-Rn	Vis	Benzyl alcohol	O_2	313	Indirect ORR	[5]
Pd/UiO-66-NH_2	Vis	No	O_2	1740	ORR	[6]
Ni/Hf-UiO-66-NH_2	Vis	No	O_2	37	Indirect ORR, WOR	[7]
C_3N_4/Ni-CAT	Vis	No	O_2	1801	Indirect ORR	[8]
$ZnIn_2S_4$/MIL-88B(Fe)–NH_2	Vis	No	Air	209	Indirect ORR	[9]
ZnS/MIL-125-NH_2	Vis	Benzyl alcohol	O_2	600	Indirect ORR	[10]
TiO_2/MIL-125-NH2/Ti_3C_2	Vis	Isopropanol	O_2	278	ORR, WOR	[11]
C/N-ZnO-NixPy	UV–vis	Ethanol	O_2	2495	ORR	[12]
TiO_2@RF	Solar	No	O_2	999	Indirect ORR	[13]
CdSe/KPN-HCP	Vis	No	O_2	900	ORR	[14]
Sulfur-Contained Resin	Salar	No	O_2	1405	ORR, WOR	[15]
D−A polymers	UV–vis	Ethanol	Air	2552.5	ORR	[16]
D–A structured BBT-ACN COF-1	Vis	No	Air	2500	Indirect ORR	[17]
π-A structured BBT-ACN COF-2	Vis	No	Air	910	Indirect ORR	[17]
Ru@Cu-HHTP	Vis	Ethanol	O_2	570.9	ORR	[18]
a Cv-PCN supramolecular	Salar	No	Air	2063.21(triphase system)	ORR	[19]

carbazole-based polymers	Vis	isopropanol	Air	1719.03	ORR	[20]
$Bi_{3.6}K_3$-CN	Vis	Ethanol	O_2	1207.72	ORR	[21]

Reference

[1] Y. Liu, S. Cui, W. Ma, et al., J. Am. Chem. Soc., 146 (2024) 12565-12576.
[2] Y. Zhao, Y. Liu, J. Cao, et al., Appl. Catal. B-Environ., 278 (2020) 119289.
[3] G. Kresse and J. Furthmu¨ller, Phys. Rev. B: Condens. Matter Mater. Phys., 1996, 54, 11169–11186.
[4] J. P. Perdew, K. Burke and M. Ernzerhof, Phys. Rev. Lett., 1996, 77, 3865–3868.
[5] Y. Isaka, Y. Kawase, Y. Kuwahara, et al., Angew. Chem. Int. Ed., 58 (2019) 5402-5406.
[6] Y.-C. Hao, L.-W. Chen, J. Li, et al., Nat. Commun., 12 (2021) 2682.
[7] Y. Kondo, K. Honda, Y. Kuwahara, et al., ACS Catal., 12 (2022) 14825-14835.
[8] Y. Zhao, Y. Liu, Z. Wang, et al., Appl. Catal. B-Environ., 289 (2021) 120035.
[9] M. Liu, Z. Xing, H. Zhao, et al., J. Hazard. Mater., 437 (2022) 129436.
[10] C. Liu, T. Bao, L. Yuan, et al., Adv. Funct. Mater., 32 (2022) 2111404.
[11] Y. Wu, X. Li, Q. Yang, et al., Chem. Eng. J., 390 (2020) 124519.
[12] A. Ray, S. Subudhi, S.P. Tripathy, et al., Adv. Mater. Inter., 9 (2022) 2201440.
[13] C. Xia, L. Yuan, H. Song, et al., Small, 19 (2023) 2300292.
[14] X. Li, B. Kang, F. Dong, et al., Nano Energy, 81 (2021) 105671.
[15] C. Zhao, H. Li, Y. Yin, et al., Angew. Chem. Int. Ed., 64 (2025) e202420895.
[16] C. Yang, Y. Xiang, W. Wang, et al., Appl. Catal. B-Environ., 365 (2025) 124856.
[17] X. Wang, H. Li, S. Zhou, et al., Adv. Funct. Mater., (2025) 2424035.
[18] C. Feng, J. Alharbi, M. Hu, et al., Adv. Mater., 37 (2025) 2406748.
[19] S. Yan, Y. Li, X. Yang, et al., Adv. Mater., 36 (2024) 2307967.
[20] X. Xia, J. Feng, Z. Zhong, et al., Adv. Funct. Mater., 34 (2024) 2311987.
[21] H. Liang, A. Wang, R. Cheng, et al., Chem. Eng. J., 489 (2024) 151145.